Acupuncture and Herbal Medicine

Corticotropin-releasing hormone neurons in the paraventricular hypothalamic nucleus modulate gastric motility *via* electroacupuncture

Yi Yuan[1], Ran Zhou[1], Juying Wang[1], Hongkun Ma[2], Hao Wang[1], Mengting Zhang[1], Shun Huang[1], Guoming Shen[1,3,*], Xiyang Wang[1,*]

[1]School of Integrated Chinese and Western Medicine, Anhui University of Chinese Medicine, Hefei, China; [2]College of Acupuncture and Moxibustion, Anhui University of Chinese Medicine, Hefei, China; [3]Institute of Health and Medicine, Hefei Comprehensive National Science Center, Hefei, China

Abstract

Objectives: Acute gastric distension (GD) impairs gastric motility and engages central stress circuits. We tested whether electroacupuncture (EA) at RN12/BL21 restores motility and probed mechanisms in the paraventricular nucleus (PVN), focusing on corticotropin-releasing hormone (CRH) neurons.

Methods: Rats underwent graded gastric balloon distension (20, 40, 60 mmHg). Gastric motility and electrogastrography determined the dysmotility threshold. Animals were randomized to EA at RN12, BL21, RN12 + BL21, or sham. PVN single-unit and local field potential activity were recorded at baseline, during GD, and after EA. Cellular Fos proto-oncogene (c-Fos)/CRH double labeling quantified PVN activation. To test causality, the CRH receptor antagonist Astressin was bilaterally microinjected into the PVN, alone or combined with EA.

Results: GD at 40 mmHg markedly suppressed gastric motility amplitude without altering slow-wave frequency, establishing this pressure as a reliable acute GD model. EA at RN12 and BL21 significantly enhanced gastric motility, with combined stimulation producing synergistic effects. GD robustly increased c-Fos expression in the PVN, including within CRH neurons, and elevated PVN neuronal firing rates and power spectral density. EA attenuated GD-induced PVN hyperactivity, reducing neuronal firing rates, power spectral energy, and local field potential activity. Immunofluorescence confirmed that EA suppressed GD-induced activation of PVN CRH neurons, with combined stimulation at RN12 and BL21 producing greater inhibition than either acupoint alone. PVN microinjection of Astressin restored gastric motility and reduced CRH neuronal activation, whereas the combination of EA and Astressin produced an additive effect on gastric motor function.

Conclusions: EA at RN12 and BL21 reverses GD-induced gastric dysmotility by dampening PVN hyperexcitability, particularly within CRH-expressing neurons. Dual-acupoint stimulation confers superior efficacy, and CRH blockade augments EA. These findings identify PVN CRH neurons as key substrates mediating EA's central control of visceral function under acute stress.

Keywords: Corticotropin-releasing hormone, Electroacupuncture, Gastric distension, Gastric motility, Hypothalamic paraventricular nucleus

Introduction

Gastric motility disorders are a hallmark of many functional gastrointestinal diseases (FGIDs), such as postprandial distress syndrome in functional dyspepsia, in which impaired gastric motility plays a central role[1]. However, therapeutic options remain limited, driving growing interest in complementary and alternative medicine (CAM)[2]. In particular, acupuncture has emerged as a promising therapeutic strategy. Meta-analyses and clinical trials suggest that electroacupuncture (EA) modulates gastric motility, gastrointestinal hormone levels, and autonomic function, offering potential benefits for patients with FGIDs[3–5].

From the perspective of traditional Chinese medicine, combining the Shu-point and Mu-point is a common clinical practice. BL21 and RN12—the Shu and Mu points of the stomach—have been shown to improve gastrointestinal dysfunction in both experimental and clinical studies[6–7]. However, the central mechanisms behind these effects remain unclear.

The hypothalamic paraventricular nucleus (PVN) is a key autonomic control center that regulates gastrointestinal function through peptidergic signaling[8–9].

Yi Yuan, Ran Zhou, and Juying Wang contributed equally to this work.

*Corresponding author. Xiyang Wang, E-mail: xiyangw1@163.com; Guoming Shen, E-mail: shengm_66@163.com.

How to cite this article: Yuan Y, Zhou R, Wang JY, Ma HK, Wang H, Zhang MT, Huang S, Shen GM, Wang XY. Corticotropin-releasing hormone neurons in the paraventricular hypothalamic nucleus modulate gastric motility via electroacupuncture. Acupunct Herb Med 2025;5(4):480–490. doi: 10.1097/HM9.0000000000000173

Received 28 February 2025 / Accepted 11 November 2025

Corticotropin-releasing hormone (CRH), a prototypical stress-related neuropeptide, is densely expressed in PVN neurons and mediates stress-induced inhibition of gastric motility[10]. Previous studies[11–13] have shown that acupuncture suppresses stress-induced CRH hyperactivity in the PVN. However, whether PVN CRH neurons are directly involved in EA-mediated regulation of gastric motility remains unclear.

In this study, we investigated the effects of EA at RN12 and BL21 on gastric motility and examined the role of PVN CRH neurons in mediating these effects. Using a combination of physiological and neurobiological approaches, we aimed to clarify the central mechanisms by which EA influences gastric function.

Materials and methods

Experimental animals

Male Sprague–Dawley rats (6–7 weeks old, 290–320 g) were housed under standard laboratory conditions (4–5 per cage) with *ad libitum* access to food and water. All experimental procedures complied with the ARRIVE guidelines[14], the U.K. Animals (Scientific Procedures) Act, and the Guidelines for the Care and Use of Laboratory Animals of Anhui University of Chinese Medicine. The protocol was approved by the Experimental Animal Certificate No. AHUCM-rats-2024224. All efforts were made to minimize animal suffering and reduce the number of animals used.

Gastric distension (GD) and motility recordings

The rats were fasted overnight with free access to water and were anesthetized on the day of the experiment using tribromoethanol (10 mL/kg, i.p.). An isobaric GD model was established using a balloon made from a 2-mm-wide latex strip attached to polyethylene tubing. The tubing was connected to a three-way stopcock, allowing simultaneous connection to a syringe and pressure transducer (MLT0380, Xinhang Xingye Technology, Beijing, China). The pressure signals were amplified using a bridge module (ML-301, AD Instruments, Dunedin, New Zealand), digitized using a PowerLab 8/30 system (AD Instruments), and analyzed offline. The lubricated balloon was advanced through the posterior pharyngeal wall into the gastric antrum and positioned at the pylorus such that its edge was sealed against the pyloric sphincter. At the end of each experiment, catheter integrity was confirmed to exclude data compromised by leakage.

Baseline pressure was defined as the mean distending pressure (MDP; ~5 mmHg)[15] achieved by inflating the balloon with saline to ensure wall apposition and then maintained at MDP + 1–2 mmHg (~6–7 mmHg) to stabilize the balloon–wall contact without mechanical interference. Continuous intragastric pressure fluctuations were recorded for the motility analysis.

Graded distension was applied at 20, 40, and 60 mmHg for 3 min each, with recovery at baseline pressure for at least 3 to 4 min between trials; a gastric pressure of 40 mmHg or higher was defined as "noxious distension" indicating successful induction of acute GD. For EA testing, 3 min of 40 mmHg distensions were delivered as pre-EA baselines. Within 20 min of the EA intervention, a 3-minute 40 mmHg distension was applied, followed by a 3- to 4-minute recovery period (Figure 1A).

For each distension, the contraction amplitude and frequency were extracted from the steady-state periods and analyzed using repeated-measures statistics. Data were processed using LabChart 8 software.

Electrogastrogram (EGG) recording

Following overnight fasting with free access to water, rats were anesthetized and positioned supine. Abdominal hair was removed, and the skin was degreased with 95% ethanol. Four Ag–AgCl electrodes were placed over the gastric antrum, gastric body, right forelimb, wrist, and right hindlimb elbow. Saline-soaked cotton balls (0.9% NaCl) were used to improve the conductivity. The gastric electrical activity was continuously recorded using a gastrogram recorder (EGEG-2D; Aoyuan Technology, Hefei, China). Recordings were obtained under three experimental conditions: baseline, GD, and GD with EA, each lasting 20 min, with at least 5 min of stabilization before data collection. Signals were digitized at a sampling rate of 100 Hz and band-pass filtered between 0.01 and 0.3 Hz to isolate gastric slow waves. Data were analyzed offline using the manufacturer's software. Gastric motility was quantified by calculating the mean amplitude (μV) and dominant frequency (cycles per minute, cpm) of the EGG during each condition.

EA stimulation

Rats were anesthetized with isoflurane 2%–2.5% and maintained on a thermostatically controlled heating pad (35.5°C–37.5°C). Stainless-steel needles (0.25 mm × 13 mm; Suzhou Medical Supplies Factory Ltd., Suzhou, China) were connected to positive and negative electrodes positioned 1 mm apart to confine stimulation to a single acupoint. Electrical stimulation was delivered using an EA device (SDZ-IV, Suzhou Medical Supplies Factory Ltd.) at 2 mA and 2 Hz for 20 min. For BL21 (Weishu), needles were inserted obliquely at a 45°angle toward the vertebral body to a depth of ~0.4 cm beneath the skin at the depression lateral to the inferior border of the 13th thoracic spinous process. For RN12 (Zhongwan), needles were inserted perpendicularly to a depth of ~0.2 cm at the midpoint between the sternum and umbilicus. Control rats received sham acupuncture at a non-acupoint on the tail, with needles inserted superficially to a depth of ~0.01 cm and without electrical stimulation (0 mA) (Figure 1B).

Immunohistochemistry and image analysis

Ninety min after the interventions, animals were anesthetized with tribromoethanol (10 mL/kg, i.p.) and perfused transcardially with 0.9% saline followed by 4% paraformaldehyde in 0.01 M phosphate-buffered saline (PBS, pH 7.4). Brains were removed, post-fixed, dehydrated, paraffin-embedded, and sectioned at 5 μm. Coronal sections containing the PVN, identified according to the rat brain atlas, were processed for

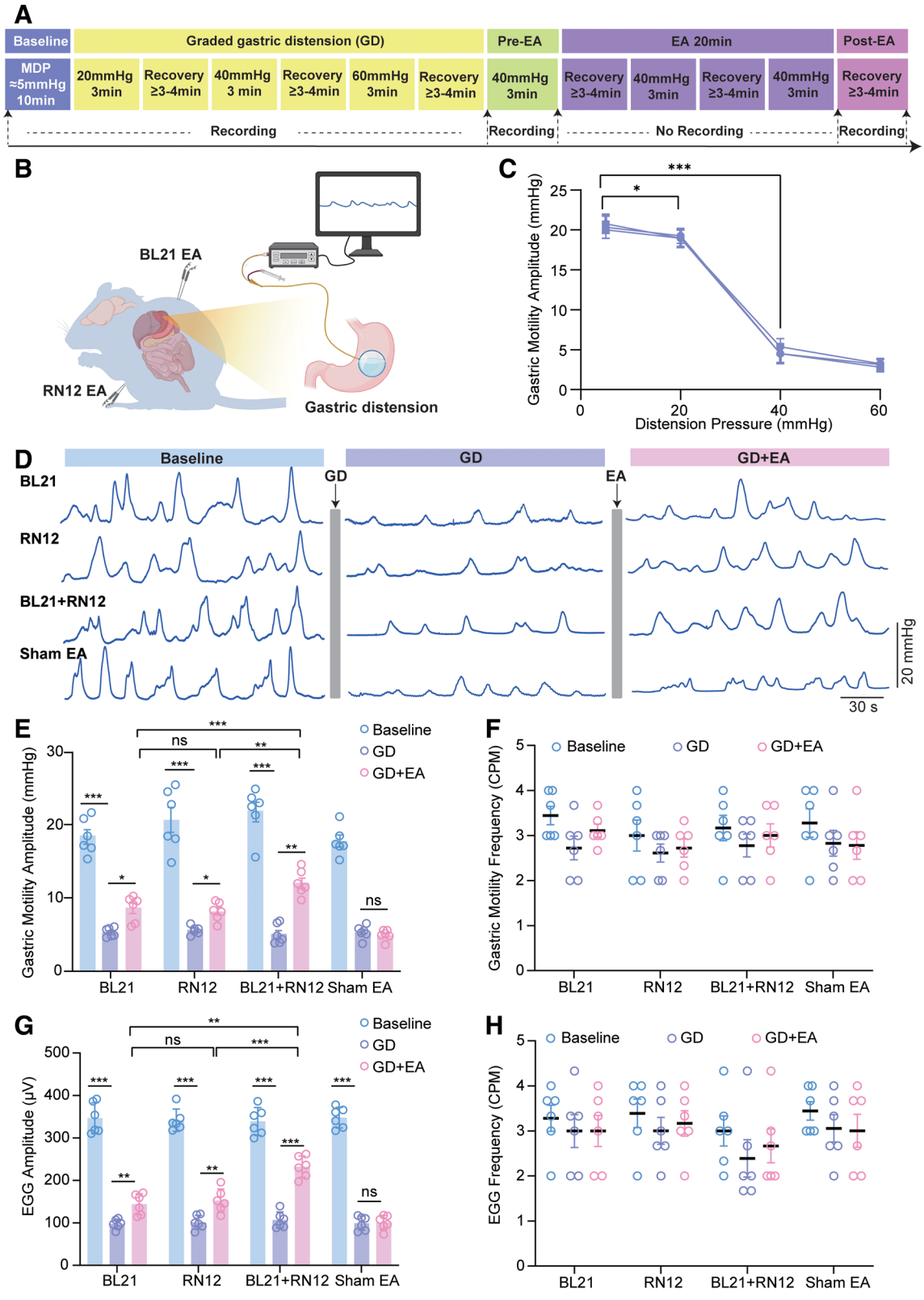

Figure 1. Electroacupuncture restores gastric motility suppressed by GD. (A) Experimental protocol. Graded GD (20/40/60 mmHg, 3 min each) was applied with recovery periods, followed by pre-EA baseline, 20 min EA (RN12 and/or BL21), and post-EA recordings. (B) Schematic of EA at RN12 and BL21 during gastric balloon distension. (C) Gastric motility amplitude progressively decreased with increasing GD pressure; 40 mmHg induced significant suppression ($n = 6$, three trials each). (D) Representative motility traces under the baseline, GD, and GD + EA conditions. (E–F) Quantification of gastric motility amplitude (E) and frequency (F) across groups (BL21, RN12, RN12 + BL21, and sham EA; $n = 6$). (G–H) EGG analyses showing amplitude (G) and frequency (H) across groups ($n = 6$). All data are presented as the mean ± SEM. *$P < 0.05$, **$P < 0.01$, ***$P < 0.001$. EA: Electroacupuncture; EEG: Electrogastrogram; GD: Gastric distension; SEM: Standard error of the mean.

immunofluorescence. Sections were incubated with primary antibodies against cellular Fos proto-oncogene (c-Fos) (mouse, 1:100; Santa Cruz, Dallas, USA, Cat# sc-166940) or CRH (rabbit, 1:100; Affinity Biosciences, Liyang, China, Cat# AF5306) for 1 hour at 37°C, followed by the appropriate secondary antibody (1:500;

Beyotime, Shanghai, China, Cat# A0428 Cat# A0468) for 30 min at 37°C. Nuclei were counterstained with 4',6-diamidino-2-phenylindole (DAPI), and slides were mounted in an anti-fade mounting medium (Beyotime Cat# P0131). Images were acquired using a fluorescence microscope (Olympus, Tokyo, Japan), and immunoreactive cells within one hemisphere of the PVN were quantified using the ImageJ software.

In vivo electrophysiology

Rats were anesthetized with 2% to 2.5% isoflurane and secured in a stereotaxic frame (RWD Life Science, Shenzhen, China). A craniotomy was performed at the PVN (anteroposterior [AP] + 1.4 mm, mediolateral [ML] + 0.3 mm, dorsoventral [DV] −7.8 mm from the dura) (Figure 3A), the dura was carefully removed, and an 8-channel microelectrode array was advanced into the PVN at 5 μm/s. The neuronal activity was recorded using a multichannel acquisition system (Plexon, Dallas, TX, USA). Single-unit firing (150–8,000 Hz; 40 kHz sampling rate) and local field potentials (0.7–400 Hz; 1 kHz sampling rate) were collected for 5 min once stable firing was observed. Data were analyzed using offline Sorter and NeuroExplorer software (Plexon).

Acute PVN microinjection protocol

The rats were fasted overnight, with free access to water. On the day of the experiment, animals were anesthetized and placed in a stereotaxic apparatus on a thermostatic heating pad. A gastric balloon was inserted, and baseline gastric motility was recorded for 10 to 15 min.

Following the injection, the animals were monitored for 10 min to allow for drug onset. Gastric motility was continuously recorded for 0 to 60 min post-injection. When required, GD was initiated 10 to 15 min after injection. For EA experiments, stimulation was applied between 15 and 25 min post-injection, followed by continued motility recordings. For immunohistochemistry, animals were perfused at ~90 min after injection, and brains were collected for c-Fos staining and histological verification of injection sites (Figure 5A). Bilateral acute microinjections were then performed into the PVN (AP + 1.4 mm, ML ± 0.3 mm, DV − 7.8 mm from the dura) using a glass micropipette connected to a microsyringe. Astressin (3.3 ng in 1 μL PBS; MedChemExpress, New Jersey, USA, Cat# HY-P0257) or vehicle was administered bilaterally at 300 nL per side, at a rate of 50 nL/min, and the injector was left in place for an additional 5 min to minimize reflux (Figure 5B).

Statistical analysis

All data are presented as mean ± standard error of the mean (SEM). Differences were analyzed with a mixed two-way analysis of variance (ANOVA) with group (RN12, BL21, RN12 + BL21, sham EA) as a between-subjects factor and state (normal, GD, and EA + GD) as a repeated measure. Sphericity was assessed (Mauchly test) and the Greenhouse–Geisser correction was applied when violated. To probe between-group differences, specifically in the EA + GD condition, we conducted simple effects tests (one-way ANOVA across groups at the EA + GD level), followed by Tukey's all-pairwise multiple-comparisons procedure. In other experiments, post-intervention amplitudes were compared among independent groups using one-way ANOVA, and when the omnibus test was significant, Tukey's *post hoc* test identified pairwise differences. Correlations were assessed with Pearson correlation, two-tailed tests with 95% confidence intervals. Statistical analyses were performed using GraphPad Prism 10; $P < 0.05$ was considered statistically significant.

Results

Synergistic effects of RN12 and BL21 stimulation on gastric motility

To establish an acute GD model, we first identified the MDP. Graded GD (20/40/60 mmHg) revealed that at 20 mmHg, gastric motility amplitude declined by 3.1% to 12.6% relative to MDP, whereas 40 mmHg reduced amplitude by 71.4% to 83.1%, and 60 mmHg by 83.3% to 90.3%. Based on these findings, 40 mmHg was selected as the threshold for acute GD (Figure 1A–C). *In vivo* electrophysiology and electrogastrography showed that GD significantly suppressed motility and disrupted gastric rhythmicity, although the slow-wave frequency remained unchanged.

We next tested whether EA at RN12 and BL21 could counteract GD-induced dysmotility and whether the combined stimulation provided additive benefits. The rats were randomized into four groups: RN12, BL21, RN12 + BL21, and sham EA. Gastric motility amplitude (Figure 1E and G) and frequency (Figure 1F and H) were measured before and 20 min after EA using *in vivo* electrophysiology and electrogastrography. EA significantly increased the motility amplitude in the RN12, BL21, and RN12 + BL21 groups compared to that in the GD state, with no effect in sham controls. Notably, combined RN12 + BL21 stimulation produced a greater recovery of motility amplitude than stimulation at either acupoint alone. Together, these results demonstrate that GD induces severe gastric dysmotility and that EA restores motility, with the dual stimulation of RN12 and BL21 exerting synergistic regulatory effects.

PVN neurons respond to GD and EA stimulation

Building on the observation that EA at RN12 and BL21 effectively restored gastric motility during acute GD, we next investigated whether hypothalamic neurons are engaged in this process. The PVN is a key integrative hub for autonomic regulation, making it a likely candidate for the mediation of gastric responses to distension and EA. To test this hypothesis, we examined the neuronal activity in the PVN using c-Fos immunohistochemistry. In the GD model group, as well as the BL21, RN12, and BL21 + RN12 groups, a substantial number of c-Fos-positive neurons were detected in the PVN. Compared to the control group, the number of c-Fos-positive neurons was significantly higher in all groups (Figure 2A and B). However, the mean fluorescence intensity (MFI) of c-Fos–positive neurons did not differ significantly

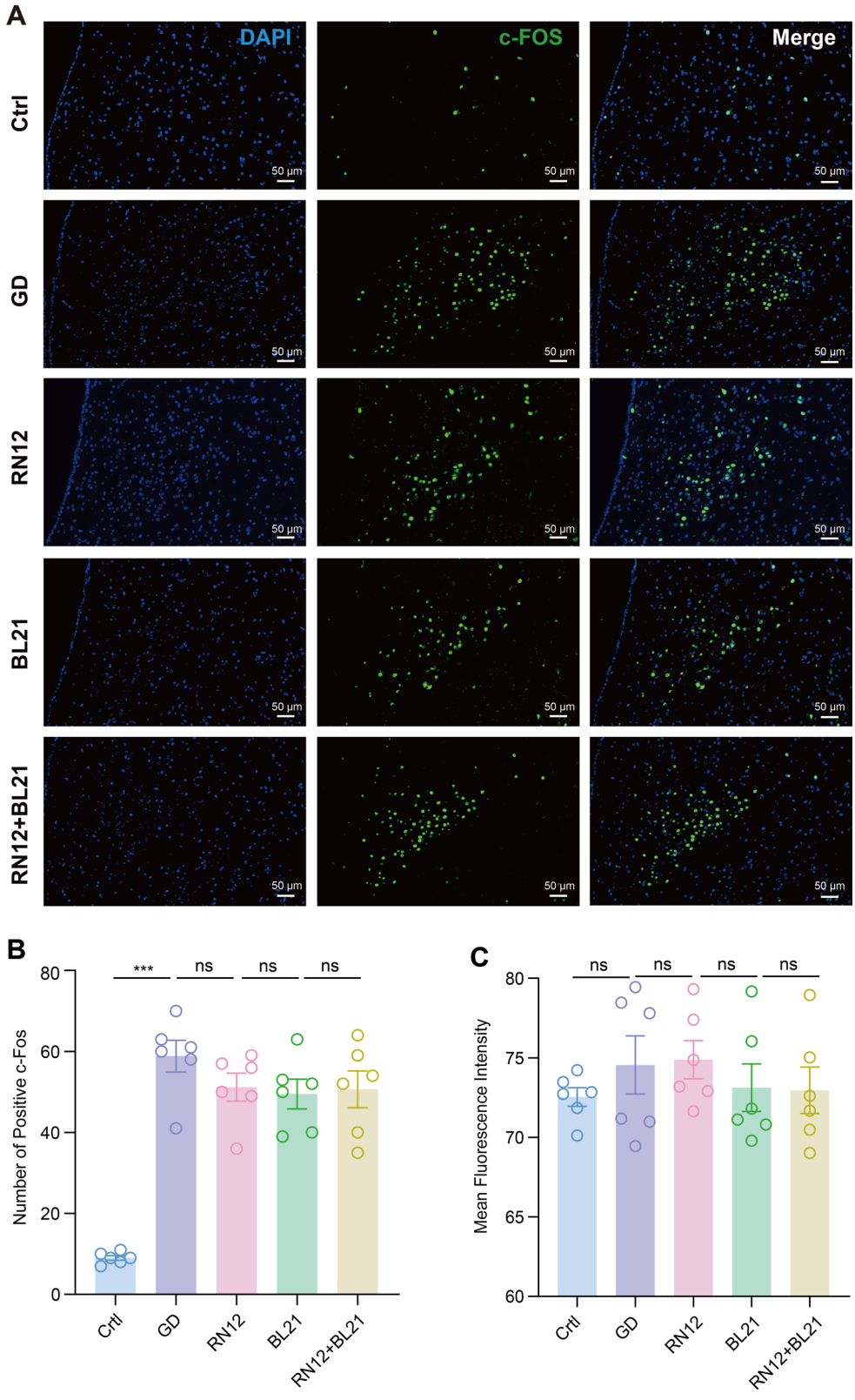

Figure 2. PVN neurons responded to GD and EA. (A) Representative immunofluorescence images of the PVN showing DAPI (blue), c-Fos (green), and merged channels in Ctrl, GD, and EA-treated groups (RN12, BL21, RN12 + BL21). Scale bar, 50 μm. (B) Quantification of c-Fos–positive neurons in the PVN across groups, $n = 6$. (C) Mean fluorescence intensity (MFI) of c-Fos–positive neurons in the PVN. c-Fos–positive neurons were auto-defined as ROIs. MFI was the 8-bit mean gray (0–255) minus the mean background from three cell-free ROIs/image. Per animal, background-corrected MFIs across sections were averaged as one replicate ($n = 6$); data shown as raw gray values. All data are presented as the mean ± SEM. ***$P < 0.001$. c-Fos: Cellular Fos proto-oncogene; Ctrl: Control; DAPI: 4',6-diamidino-2-phenylindole; EA: Electroacupuncture; GD: Gastric distension; MFI: Mean fluorescence intensity; ns: Not significant; PVN: Paraventricular nucleus; ROI: Region of interest; SEM: Standard error of the mean.

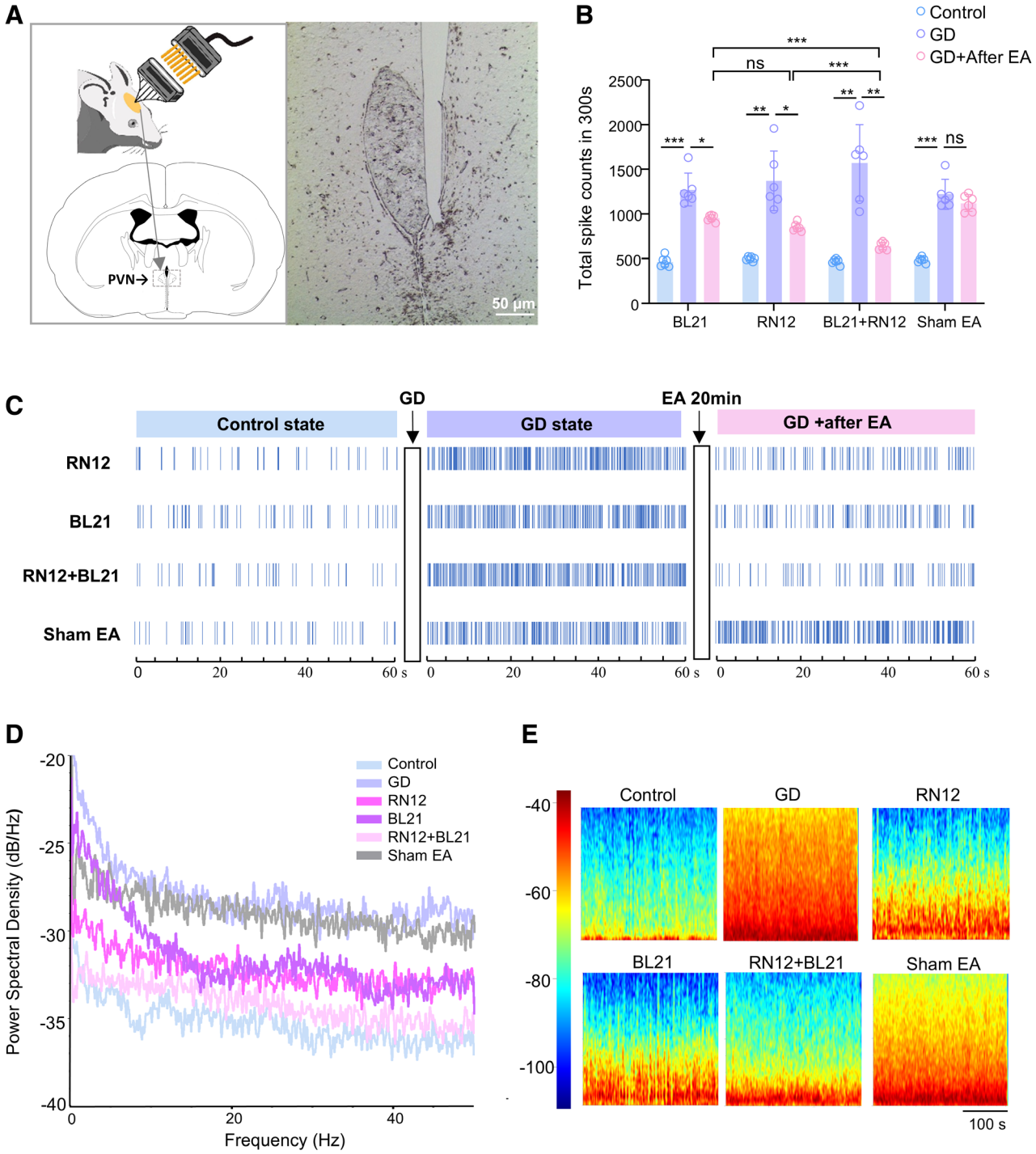

Figure 3. Electroacupuncture attenuates GD-induced hyperactivity of PVN neurons. (A) Schematic and representative histological image showing electrode placement in the PVN for *in vivo* electrophysiological recordings. Scale bar, 50 μm. (B) Quantification of total spike counts over 300 s across groups. (C) Representative raster plots of PVN neuronal firing in control, GD, and post-EA states across experimental groups. (D) PSD analysis of the control, GD, and post-EA states (RN12, BL21, RN12 + BL21, sham EA). (E) LFP spectrograms of the control, GD, and post-EA states (RN12, BL21, RN12 + BL21, and sham EA). All data are presented as the mean ± SEM. $n = 6$. *$P < 0.05$, **$P < 0.01$, ***$P < 0.001$. EA: Electroacupuncture; GD: Gastric distension; LFP: Local field potential; ns: Not significant; PSD: Power spectral density; PVN: Paraventricular nucleus; SEM: Standard error of the mean.

among groups (ns), suggesting that while more PVN neurons were recruited, the activation level of individual neurons remained comparable across conditions (Figure 2C). These findings indicate that PVN neurons are activated not only by GD but also by EA at RN12 and BL21, suggesting that the PVN may serve as a critical relay in mediating the modulatory effects of EA on gastric function.

EA attenuates PVN neuronal hyperactivity induced by GD

Given that PVN neurons are activated by both GD and EA stimulation, we sought to directly assess how neuronal firing dynamics within the PVN are modulated during these conditions. *In vivo* electrophysiological recordings provide an opportunity to capture the temporal patterns of neuronal activity at the single-cell and network levels.

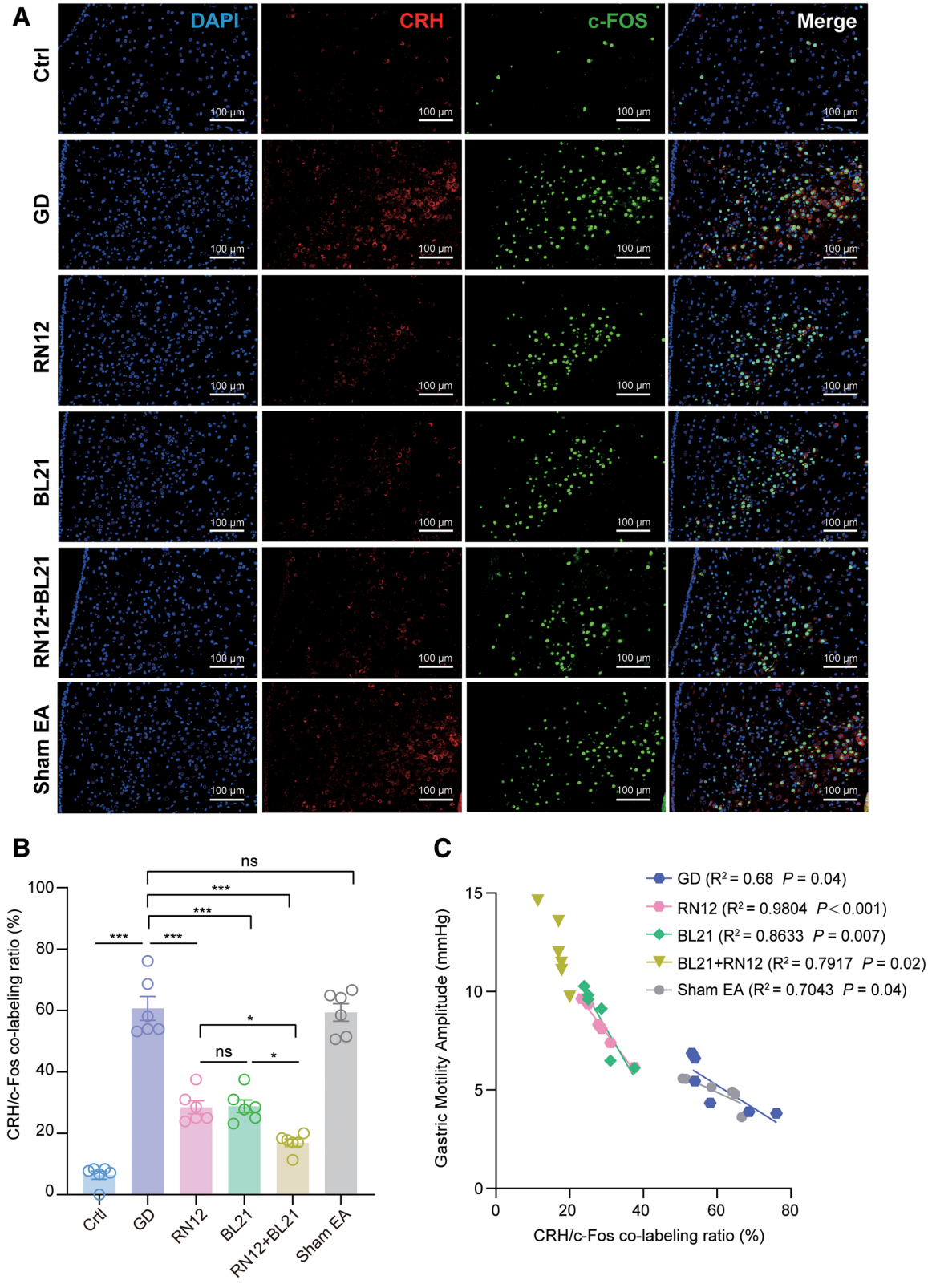

Figure 4. Electroacupuncture suppresses GD-induced activation of PVN^{CRH} neurons. (A) Representative immunofluorescence images of the PVN showing DAPI (blue), CRH (red), c-Fos (green), and merged channels across groups (Ctrl, GD, RN12, BL21, RN12 + BL21, sham EA). Scale bar, 100 μm. (B) Quantification of CRH-neuron activation in the PVN: CRH/c-Fos co-labeling ratio, defined as (c-Fos$^+$CRH$^+$ cells/total CRH$^+$ cells) × 100%. (C) Correlation analysis between PVN CRH neuronal activation (CRH/c-Fos co-labeling ratio) and gastric motility amplitude across GD, RN12, BL21, RN12 + BL21, and sham EA groups. All data are presented as the mean ± SEM. $n = 6$. *$P < 0.05$, ***$P < 0.001$. c-Fos: Cellular Fos proto-oncogene; CRH: Corticotropin-releasing hormone; Ctrl: Control; DAPI: 4',6-diamidino-2-phenylindole; EA: Electroacupuncture; GD: Gastric distension; ns: Not significant; PVN: Paraventricular nucleus; SEM: Standard error of the mean.

Using *in vivo* electrophysiological recordings, we monitored the baseline activity, GD state (pre-EA), and post-EA neuronal firing in the PVN across the experimental groups. Under GD conditions, the total firing rate of PVN neurons was significantly higher than in the normal state (Figure 3B and C). After 20 min of

EA, neuronal firing rates were markedly reduced in the RN12, BL21, and RN12 + BL21 groups, with combined RN12 + BL21 stimulation producing a greater reduction than either site alone. In contrast, the sham EA group showed no significant changes, indicating that EA effectively suppressed GD-induced PVN hyperactivity.

Power spectral density (PSD) analysis further revealed that GD markedly increased neural energy in the frequency domain across groups, whereas 20 min of EA significantly reduced PSD in the RN12, BL21, and RN12 + BL21 groups but not in the sham-EA group (Figure 3D). Similarly, the local field potential (LFP) spectral energy, which reflects the time-varying frequency characteristics of neuronal ensembles, was enhanced during GD but attenuated following EA (Figure 3E). Collectively, these findings demonstrate that EA at RN12 and/or BL21 dampens GD-induced hyperexcitability of PVN neurons, an effect not reproduced by stimulation at non-acupoints.

EA suppresses GD-activated PVN-CRH neurons

Electrophysiological data have demonstrated that EA attenuates GD-induced hyperactivity in PVN neurons. To further delineate the specific neuronal subtypes involved, we focused on CRH neurons, the predominant population within the PVN that play a pivotal role in coordinating the autonomic responses of the gastrointestinal tract under stress.

Immunofluorescence analysis revealed a striking increase in the proportion of c-Fos–positive CRH neurons in the GD group (60.64%) compared with controls (6.36%, $P < 0.001$). After 20 min of EA treatment, this activation was significantly reduced in the RN12 (26.83%), BL21 (27.18%), and RN12 + BL21 (16.53%) groups (all $P < 0.001$), whereas the sham EA group (59.37%) remained unchanged (Figure 4A and B). Notably, combined stimulation with RN12 + BL21 produced a stronger inhibitory effect on the PVN-CRH neurons than stimulation with either acupoint alone. Across groups, PVN-CRH neuronal activation was negatively correlated with gastric motility amplitude, and this correlation was observed even in the sham EA group (Figure 4C). These findings demonstrate that EA effectively suppresses the GD-induced activation of PVN-CRH neurons, with combined acupoint stimulation providing superior inhibitory effects.

CRH blockade restores gastric motility and synergizes with EA

To determine whether blockade of CRH signaling could reverse GD-induced alterations in PVN CRH neurons and gastric motility, we employed five independent groups of animals: Ctrl + Veh, GD + Veh, GD + Astressin, GD + EA + Veh, and GD + EA + Astressin. Remarkably, local microinjection of the CRH receptor antagonist Astressin modulated PVN activity and significantly restored gastric motility in GD rats, with the GD + Astressin group showing superior recovery compared with GD + Veh (Figure 5C–E). Unexpectedly, gastric myoelectrical recordings further revealed that gastric motility in the GD + EA + Astressin group was significantly stronger than that in the GD + Astressin or GD + EA + Veh groups, suggesting a synergistic interaction between CRH receptor blockade and EA (Figure 5F and G). Consistently, immunofluorescence analysis revealed a marked reduction in CRH-c-Fos co-localization within the PVN, indicating that local antagonism of CRH signaling effectively counteracted GD-induced hyperactivation (Figure 5H and I). These findings imply that EA not only exerts therapeutic effects by attenuating CRH-dependent pathways but may also engage additional mechanisms to enhance gastric motor function.

Discussion

Acute GD induces a marked suppression of gastric motility, accompanied by pronounced hyperactivation of PVN neurons, particularly CRH neurons. Here, we demonstrate that EA at RN12 and BL21 effectively restored gastric motility and attenuated PVN hyperexcitability, with combined stimulation producing the most robust effects. Furthermore, the pharmacological blockade of CRH signaling within the PVN rescues GD-induced dysmotility and acts synergistically with EA, highlighting the CRH pathway as a central substrate underlying the therapeutic effects of acupuncture.

The PVN functions as a critical integrative hub linking autonomic and endocrine control of visceral activity. It receives convergent inputs from the parabrachial complex, amygdala, bed nucleus of the stria terminalis, dorsal vagal complex (DVC), and spinal cord[16–18]. Our electrophysiological and immunofluorescence data demonstrate that GD induces PVN hyperactivity, whereas EA normalizes this state, supporting the role of the PVN as a key relay in the regulation of gastric function.

Stress-related gastrointestinal disorders are closely linked to CRH signaling. Within the PVN, CRH neurons release CRH to brainstem nuclei, such as the DVC, where they modulate the output of the dorsal motor nucleus of the vagus and inhibit gastric motility[9,19–21]. This pathway has been implicated in functional dyspepsia and other stress-related gastric disorders[22–23]. In line with this framework, we observed that EA markedly suppressed GD-induced activation of PVN CRH neurons, suggesting that acupuncture alleviates gastric dysfunction, at least in part, by inhibiting stress-responsive CRH signaling. Notably, PVN CRH neuronal activation was negatively correlated with gastric motility amplitude, a trend observed even in the sham EA group. This indicates that the observed negative correlation reflects the intrinsic inhibitory role of CRH neurons on gastric motility, rather than a specific effect of EA. Consequently, the modulation of PVN CRH neurons by EA may restore gastric function by rebalancing central stress circuits, highlighting a mechanistic link between central CRH signaling and visceral motor output.

Previous studies have reported that GD activates hypothalamic stress circuits and disrupts gastric motor function, whereas acupuncture enhances gastrointestinal motility under both physiological and pathological conditions[24–26]. Our findings extend this body of work by demonstrating that dual Shu–Mu acupoint stimulation

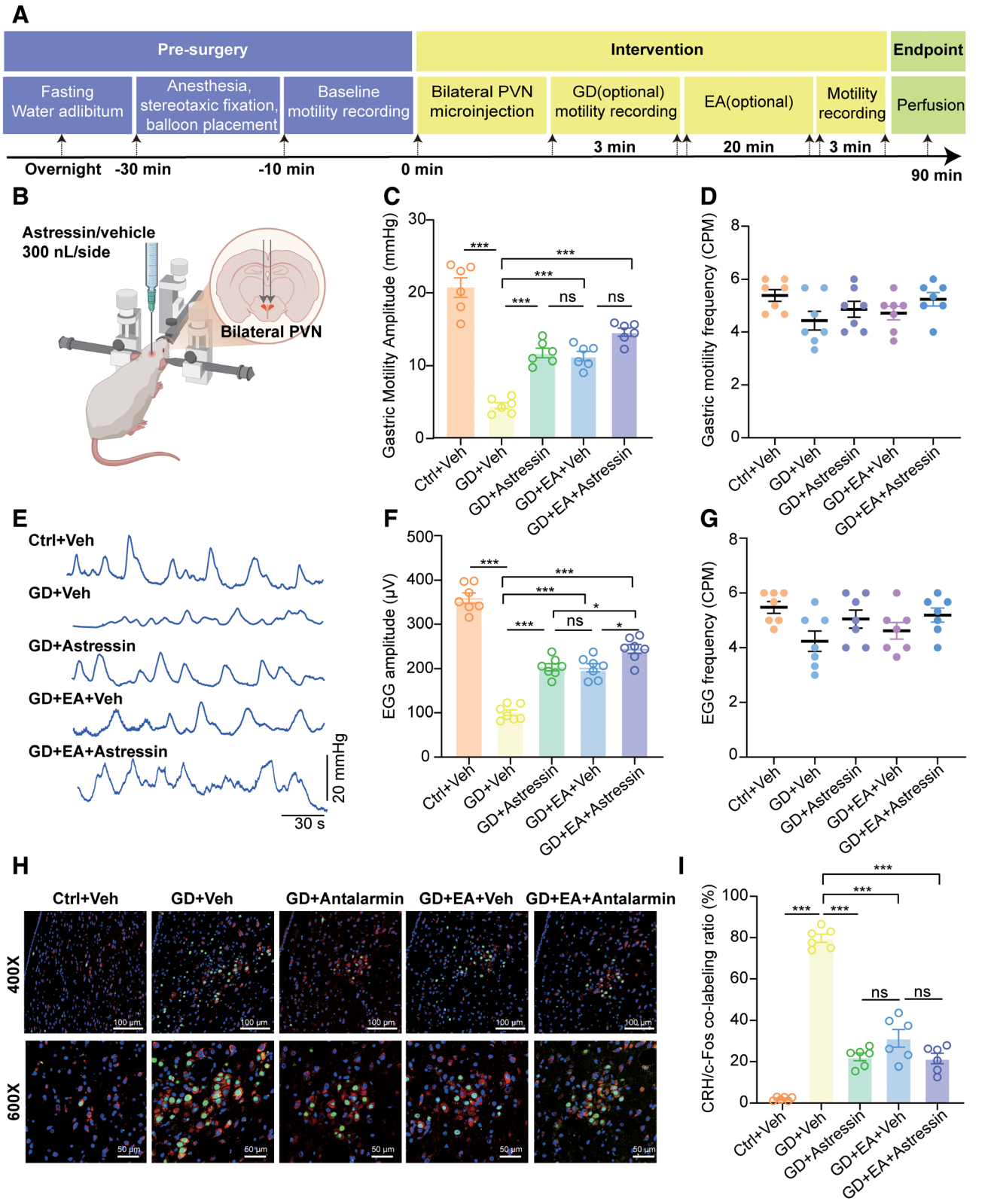

Figure 5. CRH receptor blockade restores gastric motility and synergizes with electroacupuncture. (A) Experimental timeline. Rats underwent overnight fasting, anesthesia, stereotaxic fixation, gastric balloon placement, and baseline motility recording, followed by GD and motility recordings (as applicable to each group). EA was applied for 20 min, after which post-EA gastric motility was recorded. Perfusion was performed 90 min after microinjection. (B) Schematic of bilateral PVN microinjection (300 nL/side) of Astressin or vehicle. (C–D) EGG analysis showing amplitude (C) and frequency (D) across groups. (E) Representative traces of gastric motility under the indicated conditions. (F–G) Quantification of gastric motility amplitude (F) and frequency (G). Astressin significantly restored motility amplitude in GD rats, and combined EA + Astressin produced additive improvements, whereas frequency remained unaffected. (H) Representative immunofluorescence images of PVN neurons showing c-Fos (green) and CRH (red) under each condition at 400× and 600× magnifications. Scale bars: 100 and 50 μm. (I) Quantification of CRH-neuron activation in the PVN: CRH/c-Fos co-labeling ratio, defined as (c-Fos$^+$CRH$^+$cells/total CRH$^+$ cells) × 100%. All data are presented as mean ± SEM; $n = 6$. *$P < 0.05$, ***$P < 0.001$. c-Fos: Cellular Fos proto-oncogene; CRH: Corticotropin-releasing hormone; Ctrl: Control; EA: Electroacupuncture; EGG: Electrogastrography; GD: Gastric distension; ns: Not significant; PVN: Paraventricular nucleus; SEM: Standard error of the mean.

(RN12 + BL21) exerts more pronounced modulatory effects than single-site stimulation, which is consistent with clinical evidence[5] and basic research[16,24] suggesting that compatible acupoint combinations yield superior outcomes in functional dyspepsia. The observed synergy between EA and CRH blockade further suggests that acupuncture acts not only through CRH-dependent mechanisms but also *via* additional PVN microcircuits and vagal pathways, thereby maximizing its regulatory impact on gastric motor function.

These results identify CRH neurons in the PVN as key mediators of EA-induced regulation of gastric motility. Given the established role of CRH signaling in stress-related gut dysfunction, our findings provide a neurobiological rationale for the clinical benefits of acupuncture in conditions such as functional dyspepsia. Moreover, the synergy between EA and CRH antagonism suggests that combined pharmacological and neuromodulatory strategies could offer an effective approach to restoring gastric homeostasis in stress-sensitive patients.

Although our study focused on CRH neurons, the PVN is a heterogeneous nucleus containing oxytocin, vasopressin, glutamatergic, and GABAergic neurons, all of which contribute to visceral regulation[27–28]. Oxytocin neurons projecting to the DVC enhance vagal drive and facilitate gastric motility, while vasopressin neurons influence autonomic outflow[29–30], and local GABAergic interneurons modulate the excitability of CRH neurons[31]. Therefore, EA may influence a broader PVN microcircuit[32]. Future studies employing cell-type-specific manipulations such as optogenetics or chemogenetics are required to dissect the distinct contributions of these neuronal populations.

Our study is limited by its reliance on an acute GD rat model, which may not fully capture the complexity of chronic human gastrointestinal disorders. Moreover, although our results strongly implicate CRH neurons, causal confirmation requires the selective manipulation of CRH and non-CRH PVN subtypes. Future studies using chronic models, cell-specific approaches, and translational research will be necessary to establish the therapeutic relevance of these findings. Nevertheless, by demonstrating that EA suppresses GD-induced CRH hyperactivity and that CRH antagonism potentiates EA, we provide mechanistic evidence that acupuncture acts through both CRH-dependent and CRH-independent pathways within the PVN. This cellular-level insight advances our understanding of the gut–brain axis and supports EA as a promising intervention for stress-related gastric dysmotility.

Conflict of interest statement

The authors declare no conflict of interest.

Funding

This work was supported by the Young Scientists Fund of the National Natural Science Foundation of China (82405244), the National Natural Science Foundation of China (82474224), the Center for Xin'an Medicine and Modernization of Traditional Chinese Medicine at IHM (2023CXMMTCM016), and the National Training Program of Innovation for Undergraduates (20251036961).

Author contributions

Material preparation, data collection, and analysis were carried out by Xiyang Wang, Yi Yuan, Ran Zhou, Juying Wang, and Hongkun Ma. Supplementary experiments were conducted by Ran Zhou and Juying Wang. The first draft of the manuscript was written by Xiyang Wang, with the study conceptualized by Xiyang Wang and Guoming Shen. Manuscript review and editing were performed by Mengting Zhang, Ran Zhou, and Juying Wang. Hao Wang and Shun Huang supervised the project, and funding was provided by Xiyang Wang and Guoming Shen.

Ethical approval of studies and informed consent

All experiments were conducted in accordance with the ARRIVE guidelines and were approved by the Animal Experimentation Ethics Committee of Anhui University of Traditional Chinese Medicine (Reference No. AHUCM-rats-2024224).

Acknowledgments

We thank all co-authors for their valuable contributions to this study. Schematic figures were prepared using BioRender.com.

Data availability

All data generated or analyzed during this study are included in this published article.

References

[1] Shin A. Disorders of gastric motility. *Lancet Gastroenterol Hepatol* 2024;9(11):1052–1064.
[2] Deutsch JK, Levitt J, Hass DJ. Complementary and alternative medicine for functional gastrointestinal disorders. *Am J Gastroenterol* 2020;115(3):350–364.
[3] Guo Y, Wei W, Chen JD. Effects and mechanisms of acupuncture and electroacupuncture for functional dyspepsia: a systematic review. *World J Gastroenterol* 2020;26(19):2440–2457.
[4] Wang L, Xian J, Sun M, et al. Acupuncture for emotional symptoms in patients with functional gastrointestinal disorders: a systematic review and meta-analysis. *PLoS One* 2022;17(1):e0263166.
[5] Wang L, Luo X, Qing X, et al. Symptom effects and central mechanism of acupuncture in patients with functional gastrointestinal disorders: a systematic review based on fMRI studies. *BMC Gastroenterol* 2024;24(1):47.
[6] Wang H, Liu WJ, Hu MJ, et al. Acupuncture at Gastric Back-Shu and Front-Mu acupoints enhances gastric motility *via* the inhibition of the glutamatergic system in the hippocampus. *Evid Based Complement Alternat Med* 2020;2020:3524641.
[7] Li L, Zang H, Jiang Y, et al. Acupuncture at Back-Shu and Front-Mu acupoints prevents gastric ulcer by regulating the TLR4/MyD88/NF-κB signaling pathway. *Evid Based Complement Alternat Med* 2021;2021:8214052.
[8] Carson KE, Alvarez J, Mackley JQ, et al. Perinatal high-fat diet exposure alters oxytocin and corticotropin releasing factor inputs onto vagal neurocircuits controlling gastric motility. *J Physiol* 2023;601(14):2853–2875.
[9] Rasiah NP, Loewen SP, Bains JS. Windows into stress: a glimpse at emerging roles for CRH(PVN) neurons. *Physiol Rev* 2023;103(2):1667–1691.

[10] Filaretova LP, Morozova OY, Yarushkina NI. Peripheral corticotropin-releasing hormone may protect the gastric musosa against indometacin-induced injury through involvement of glucocorticoids. *J Physiol Pharmacol* 2021;72(5):771–720.
[11] He F, Wang M, Geng X, et al. Effect of electroacupuncture on the activity of corticotrophin-releasing hormone neurons in the hypothalamus and amygdala in rats exposed to restraint water-immersion stress. *Acupunct Med* 2018;36(6):394–400.
[12] Zheng J, Wang Y, Zhang C, et al. Electroacupuncture negatively regulates the Nesfatin-1/ERK/CREB pathway to alleviate HPA axis hyperactivity and anxiety-like behaviors caused by surgical trauma. *Chin Med* 2024;19(1):108.
[13] Zhou J, Zhang B, Zhou X, et al. Electroacupuncture pretreatment mediates sympathetic nerves to alleviate myocardial ischemia-reperfusion injury *via* CRH neurons in the paraventricular nucleus of the hypothalamus. *Chin Med* 2024;19(1):43.
[14] Percie du Sert N, Hurst V, Ahluwalia A, et al. The ARRIVE guidelines 2.0: updated guidelines for reporting animal research. *Br J Pharmacol* 2020;177(16):3617–3624.
[15] Römer M, Painsipp E, Schwetz I, et al. Facilitation of gastric compliance and cardiovascular reaction by repeated isobaric distension of the rat stomach. *Neurogastroenterol Motil* 2005;17(3):399–409.
[16] Wang XY, Chen XQ, Wang GQ, et al. A neural circuit for gastric motility disorders driven by gastric dilation in mice. *Front Neurosci* 2023;17:1069198.
[17] Zhang FC, Weng RX, Li D, et al. A vagus nerve dominant tetra-synaptic ascending pathway for gastric pain processing. *Nat Commun* 2024;15(1):9824.
[18] Li YW, Li W, Wang ST, et al. The autonomic nervous system: a potential link to the efficacy of acupuncture. *Front Neurosci* 2022;16:1038945.
[19] Li H, Page AJ. Altered vagal signaling and its pathophysiological roles in functional dyspepsia. *Front Neurosci* 2022;16:858612.
[20] Bonaz B, Sinniger V, Pellissier S. Role of stress and early-life stress in the pathogeny of inflammatory bowel disease. *Front Neurosci* 2024;18:1458918.
[21] Chaves T, Fazekas CL, Horváth K, et al. Stress adaptation and the brainstem with focus on corticotropin-releasing hormone. *Int J Mol Sci* 2021;22(16):9090.
[22] Xu Z, Zhang X, Shi H, et al. Efficacy of acupuncture for anxiety and depression in functional dyspepsia: a systematic review and meta-analysis. *PLoS One* 2024;19(3):e0298438.
[23] Liao X, Tian Y, Zhang Y, et al. Acupuncture for functional dyspepsia: Bayesian meta-analysis. *Complement Ther Med* 2024;82:103051.
[24] Wang H, Liu WJ, Wang XY, et al. A central amygdala input to the dorsal vagal complex controls gastric motility in mice under restraint stress. *Front Physiol* 2023;14:1074979.
[25] Yu Z. Neuromechanism of acupuncture regulating gastrointestinal motility. *World J Gastroenterol* 2020;26(23):3182–3200.
[26] Zhang Z, Li R, Chen Y, et al. Integration of traditional, complementary, and alternative medicine with modern biomedicine: the scientization, evidence, and challenges for integration of traditional Chinese medicine. *Acupunct Herb Med* 2023;4(1):68–78.
[27] Pyner S. Neurochemistry of the paraventricular nucleus of the hypothalamus: implications for cardiovascular regulation. *J Chem Neuroanat* 2009;38(3):197–208.
[28] Berkhout JB, Poormoghadam D, Yi C, et al. An integrated single-cell RNA-seq atlas of the mouse hypothalamic paraventricular nucleus links transcriptomic and functional types. *J Neuroendocrinol* 2024;36(2):e13367.
[29] Jiang Y, Travagli RA. Hypothalamic-vagal oxytocinergic neurocircuitry modulates gastric emptying and motility following stress. *J Physiol* 2020;598(21):4941–4955.
[30] Xia J, Zou Y, Cui Y, et al. Physical exercise activates a PVN-NAc oxytocin circuit to relieve stress-induced depressive-like behaviors. *Proc Natl Acad Sci USA* 2025;122(21):e2503675122.
[31] McIntyre C, Li XF, Ivanova D, et al. Hypothalamic PVN CRH neurons signal through PVN GABA neurons to suppress GnRH pulse generator frequency in female mice. *Endocrinology* 2023;164(6):bqad075.
[32] Guo Z, Wei N, Ye R, et al. Map activation of various brain regions using different frequencies of electroacupuncture ST36, utilizing the FosCreER strategy. *Acupunct Herb Med* 2024;4(3):386–398.